

# Unexpected transition from single to double quantum well potential induced by intense laser fields in a semiconductor quantum well

Cite as: J. Appl. Phys. **105**, 123111 (2009); <https://doi.org/10.1063/1.3153963>

Submitted: 17 February 2009 . Accepted: 18 May 2009 . Published Online: 26 June 2009

F. M. S. Lima, M. A. Amato, O. A. C. Nunes, A. L. A. Fonseca, B. G. Enders, and E. F. da Silva



View Online



Export Citation

## ARTICLES YOU MAY BE INTERESTED IN

**Electronic and intraband optical properties of single quantum rings under intense laser field radiation**

Journal of Applied Physics **116**, 093101 (2014); <https://doi.org/10.1063/1.4894446>

**Linear and nonlinear optical absorption coefficients and refractive index changes in spherical quantum dots: Effects of impurities, electric field, size, and optical intensity**

Journal of Applied Physics **103**, 073512 (2008); <https://doi.org/10.1063/1.2904860>

**Dichotomy of the exciton wave function in semiconductors under intense laser fields**

Journal of Applied Physics **103**, 113112 (2008); <https://doi.org/10.1063/1.2937087>

**HIDEN**  
ANALYTICAL

## Instruments for Advanced Science

Contact Hiden Analytical for further details:

W [www.HidenAnalytical.com](http://www.HidenAnalytical.com)  
E [info@hiden.co.uk](mailto:info@hiden.co.uk)

CLICK TO VIEW our product catalogue



### Gas Analysis

- dynamic measurement of reaction gas streams
- catalysis and thermal analysis
- molecular beam studies
- dissolved species probes
- fermentation, environmental and ecological studies



### Surface Science

- UHV TPD
- SIMS
- end point detection in ion beam etch
- elemental imaging - surface mapping



### Plasma Diagnostics

- plasma source characterization
- etch and deposition process reaction kinetic studies
- analysis of neutral and radical species



### Vacuum Analysis

- partial pressure measurement and control of process gases
- reactive sputter process control
- vacuum diagnostics
- vacuum coating process monitoring

# Unexpected transition from single to double quantum well potential induced by intense laser fields in a semiconductor quantum well

F. M. S. Lima,<sup>1,a)</sup> M. A. Amato,<sup>2</sup> O. A. C. Nunes,<sup>2</sup> A. L. A. Fonseca,<sup>2</sup> B. G. Enders,<sup>2</sup> and E. F. da Silva, Jr.<sup>1</sup>

<sup>1</sup>*Departamento de Física, Universidade Federal de Pernambuco, 50670-901 Recife-PE, Brazil*

<sup>2</sup>*Instituto de Física, Universidade de Brasília, P.O. Box 04455, 70919-970 Brasília-DF, Brazil*

(Received 17 February 2009; accepted 18 May 2009; published online 26 June 2009)

When an electronic system is irradiated by an intense laser field, the potential “seen” by electrons is modified, which affects significantly the bound-state energy levels, a feature that has been observed in transition energy experiments. For lasers for which the dipole approximation applies, a nonperturbative approach based upon the Kramers–Henneberger translation transformation, followed by Floquet series expansions, yields, for sufficiently high frequencies, the so-called “laser-dressed” potential, which is taken for composing a time-independent Schrödinger equation whose solutions are the desired quasistationary states. This approach, developed originally for atoms, has been verified to be useful also for carriers in semiconductor nanostructures under intense laser fields. In quantum wells, analytical expressions for the dressed potential have been proposed in literature for a nonresonant, intense laser field polarized perpendicularly to the interfaces. By noting that they apply only for  $\alpha_0 \leq L/2$ , where  $\alpha_0$  is the *laser-dressing parameter* and  $L$  is the well width, we derive here an analytical expression valid for all values of  $\alpha_0$ . Interestingly, our model predicts the formation of a double-well potential for laser frequencies and intensities such that  $\alpha_0 > L/2$ , which creates a possibility of generating resonant states into the channel. In addition, the rapid coalescence of the energy levels with the increase in  $\alpha_0$  we found indicates the possibility of controlling the population inversion in quantum well lasers operating in the optical pumping scheme. © 2009 American Institute of Physics. [DOI: 10.1063/1.3153963]

## I. INTRODUCTION

The understanding of the effects of external electromagnetic (EM) fields on the optical and transport properties of low-dimensional systems—e.g., electrons confined in semiconductor nanostructures—is crucial for the evolution of the emerging *nanoelectronics*, an area that has attracted increasing interest due to the possibilities it opens in applied physics.<sup>1</sup> As is well known, the application of either an electrostatic (Franz–Keldysh and quantum confined Stark effects) or a magnetic field (Shubnikov–de Haas oscillations and quantum Hall effects) changes the quantum states of carriers confined in nanostructures.<sup>2,3</sup> Recently, the development of high-power tunable laser sources, such as free-electron lasers (FELs), has fueled research activities on the interaction of intense laser fields (ILFs) with carriers in semiconductor nanostructures.<sup>4</sup> This has allowed the discovery of interesting physical phenomena such as changes in the electron density of states (DOS) in quantum wells (QWs) and quantum wires via the dynamical Franz–Keldysh effect (DFKE),<sup>5–7</sup> the measurement of zero-resistance states in two-dimensional electron gases under microwave radiation,<sup>8</sup> changes in the energy bandgap in semiconductors,<sup>9</sup> strong distortions in the optical absorption spectra,<sup>10</sup> terahertz resonant absorption in QWs,<sup>11</sup> and Floquet–Bloch states in single-walled carbon nanotubes,<sup>12</sup> among others.

In QWs, the problem of estimating the effects of a high-frequency ILF on the confining potential and the correspond-

ing bound states plays an important role in the models developed for studying, e.g., the tuning of QW lasers,<sup>13</sup> resonant tunneling,<sup>14</sup> electron DOS,<sup>6</sup> hydrogenic impurity states,<sup>15–20</sup> intersubband transitions,<sup>21</sup> and interband (electron-hole) radiative recombination.<sup>22,23</sup> For electrons confined in a rectangular QW irradiated by a nonresonant ILF polarized perpendicularly to the heterointerfaces, the nonperturbative approach based upon the Kramers–Henneberger (KH) translation transformation soon revealed that for sufficiently high frequencies, the zeroth order term of the Fourier–Floquet series expansion of the potential dominates, the so-called “laser-dressed” potential.<sup>13,15</sup> For describing this potential, some simple analytical expressions have been proposed.<sup>15–17,20</sup> Most of these works make use of the approximation suggested by Ehlötzky,<sup>24</sup> within which the integral expression for the dressed potential can be solved straightforwardly. However, in some recent works it has been shown that this approximation is, in fact, unnecessary in rectangular QWs since, in this system, that integral can be solved analytically.<sup>6,18,19,22</sup> The walls of the potential well are then predicted to assume curved profiles that distort more and more with the increase in  $\alpha_0$ , the *laser-dressing parameter* (a laser parameter that depends upon both the laser frequency and intensity). We have noted that all these expressions are valid only for  $\alpha_0 \leq L/2$ ,  $L$  being the well width. Since the current laser technology yields laser beams for which  $\alpha_0$  easily reaches tens of nanometers, a systematic investigation of the energy shifts for all bound states and the exploration of cases for which  $\alpha_0 > L/2$  are sought. The lack

<sup>a)</sup>Electronic mail: fabio@fis.unb.br.

in such theoretical studies in literature may be due to the fact that all energy levels are equally blueshifted in the DFKE effect (see Refs. 5 and 6) and to the belief that the range  $\alpha_0 > L/2$  does not bring any novelty to the physics of QWs under ILFs.

We investigate here how a linearly polarized, nonresonant ILF affects the potential well and the corresponding bound states for electrons in a single semiconductor QW. For sufficiently high frequencies, a closed-form expression for the dressed potential valid for all  $\alpha_0 > 0$  is presented. Interestingly, for  $\alpha_0 > L/2$ , the formation of a double-well potential is predicted. The coalescence of the energy levels found for a GaAs/AlGaAs QW with the increase in  $\alpha_0$  indicates the possibility of enhancing the population inversion in a QW laser that operates via optical pumping. The possibility of creation of controllable resonant states located only in the well material layer is also pointed out.

## II. THEORY FOR ELECTRONS IN A QW UNDER HIGH-FREQUENCY ILFS

In the absence of external fields, a single QW potential is seen by carriers confined in a sandwiched heterostructure composed of a layer of semiconductor A with width  $L$  involved with thick layers of a semiconductor B with a larger bandgap. We assume abrupt barriers at  $z = \pm \ell$ , where  $\ell \equiv L/2$ . We choose the  $z$ -axis along the growth direction (i.e., perpendicularly to the heterointerfaces). For a nominally undoped heterostructure, a rectangular QW is formed, which is described synthetically by  $V_b(z) = V_0 \times \Theta(|z| - \ell)$ , where  $\Theta(x)$  is the Heaviside unit step function and  $V_0$  is the (finite) depth of the potential well, corresponding to the conduction-band offset between semiconductors A and B. In the frame of non-relativistic quantum mechanics, within the effective-mass approximation, the electronic wave function is separable into a product of two factors, one for the in-plane motion (free) and the other for the motion along the  $z$ -axis direction, as given by  $\Psi(\mathbf{p}, z) = \exp(i\mathbf{k}_\perp \cdot \mathbf{p}) \times \chi(z)$ , where  $\mathbf{k}_\perp$  is the in-plane wavevector,  $\mathbf{p} = x\hat{x} + y\hat{y}$ , and  $\chi(z)$  is the wave function for the motion along the  $z$ -axis. By assuming a uniform effective mass  $m^*$  and a parabolic conduction band,<sup>25</sup> the total energy is  $\varepsilon = k_\perp^2 / (2m^*) + E_n$ , where  $E_n$  is the energy eigenvalue associated with the eigenfunction  $\chi_n(z)$  for the  $n$ th subband, which satisfies the following time-independent Schrödinger (SCD) equation:  $-(\hbar^2/2m^*)(d^2\chi_n/dz^2) + V_b(z)\chi_n(z) = E_n\chi_n(z)$ .<sup>2</sup> The exact solution of this equation in each layer yields the following set of eigenfunctions:

$$\chi_n(z) = \begin{cases} (-1)^n B e^{\kappa_b(z+\ell)}, & z \leq -\ell \\ A f(\kappa z), & |z| < \ell \\ B e^{-\kappa_b(z-\ell)}, & z \geq +\ell, \end{cases} \quad (1)$$

where  $\kappa \equiv \sqrt{2m^*E_n}/\hbar$ ,  $\kappa_b \equiv \sqrt{2m^*(V_0 - E_n)}/\hbar$ ,  $f(x) = \cos x$  ( $\sin x$ ) for  $n$  even (odd), and both  $A$  and  $B$  are normalization constants.<sup>2,3</sup> The  $N+1$  distinct eigenvalues  $E_n$  ( $n = 0, 1, \dots, N$ ) are easily found as the successive numerical solutions of the transcendental equations that come from the usual matching conditions for  $\chi_n(z)$  and its derivative at the interfaces, namely,<sup>26</sup>

$$\frac{\kappa_b}{\kappa} = \begin{cases} \tan(\kappa\ell), & n \text{ even} \\ -\cot(\kappa\ell), & n \text{ odd}. \end{cases} \quad (2)$$

The number of bound eigenstates can be anticipated as  $N = \text{Int}(\kappa_0 L / \pi)$ , where  $\kappa_0 \equiv \sqrt{2m^*V_0}/\hbar$ .

When this QW is irradiated by a monochromatic, nonresonant EM radiation field linearly polarized along the  $z$ -axis direction,<sup>27</sup> the electronic states under the combined forces of the QW potential and the EM field can be studied by including the potential corresponding to the external EM field in the kinetic part of the Hamiltonian operator. This is done here semiclassically by combining a quantum description of the particle motion with a classical description of the radiation field,<sup>28</sup> which yields the following time-dependent SCD equation:

$$\left\{ \frac{[\mathbf{p} + e\mathbf{A}]^2}{2m^*} + V_b(z) \right\} \psi(z, t) = i\hbar \frac{\partial \psi(z, t)}{\partial t}, \quad (3)$$

where  $\mathbf{p} = -i\hbar\nabla$  is the momentum operator and  $\mathbf{A} = \mathbf{A}(z, t)$  is the vector potential for the EM field. For fields that do not vary significantly in the physically important region of space, the dipole approximation applies and  $\mathbf{A}(z, t) \approx \mathbf{A}(t)$ .<sup>29</sup> In the Coulomb gauge, this EM field is related to the vector potential through  $\mathbf{F} = -\partial\mathbf{A}/\partial t$ . For any oscillatory  $\mathbf{A}(t)$ , one can perform the KH unitary translation transformation on Eq. (3) in order to transfer the time dependence from the kinetic to the potential term in the Hamiltonian operator at the left-hand side of this equation. By doing  $\varphi(z, t) = U^\dagger \psi(z, t)$  and  $\tilde{H} = U^\dagger H U$ , where

$$U = \exp \left[ -\frac{i}{\hbar} \left( \frac{e}{m^*} \int \mathbf{A} \cdot \mathbf{p} dt + \frac{e^2}{2m^*} \int \mathbf{A}^2 dt \right) \right] \quad (4)$$

is the operator for the KH transformation and  $H$  is the Hamiltonian,<sup>30–32</sup> Eq. (3) becomes<sup>6,33</sup>

$$\left\{ \frac{\mathbf{p}^2}{2m^*} + V_b[z + \alpha(t)] \right\} \varphi(z, t) = i\hbar \frac{\partial \varphi(z, t)}{\partial t}, \quad (5)$$

where  $\alpha(t) = e/m^* \int^t A(t') dt'$ .<sup>34</sup> For simplicity, let us assume a monochromatic EM field with harmonic dependence on  $t$ , i.e.,  $\mathbf{A}(t) = A_0 \cos(\omega t) \hat{z}$ , where  $A_0 = F_0/\omega$ ,  $F_0$  being the field strength. For this field, one has  $\alpha(t) = \alpha_0 \sin(\omega t)$ , with  $\alpha_0 \equiv eF_0/(m^*\omega^2)$ .<sup>34</sup> Equation (5) reflects the fact that the electron motion in the presence of an EM field can be alternatively described in an accelerated frame that oscillates in phase to the field—i.e., the Kramers frame—in which the electrons interact with the oscillating potential  $V_b[z + \alpha(t)] = V_0 \times \Theta[|z + \alpha_0 \sin(\omega t)| - \ell]$ .<sup>35,36</sup> This periodic potential can be expanded in a Fourier–Floquet series and, for sufficiently high frequencies, the zeroth order term dominates.<sup>35,36</sup> This term corresponds to the time average  $1/T \int_0^T V_b[z + \alpha(t)] dt$ , where  $T = 2\pi/\omega$  is the period of the radiation field.<sup>6,15,36</sup> This is just the *laser-dressed potential* associated with the rectangular QW potential.<sup>37</sup> In the intervals  $-\ell - \alpha_0 \leq z \leq -\ell + \alpha_0$  and  $\ell - \alpha_0 \leq z \leq \ell + \alpha_0$ , it was already shown in Refs. 18 and 22 that this integral can be solved analytically, resulting in  $V_0/\pi \times \arccos[(\ell - |z|)/\alpha_0]$  and  $-V_0/\pi \times \arcsin[(z + \ell)/\alpha_0]$ , respectively. However, we have noted that these simple expressions are valid only for  $\alpha_0 \leq \ell$ . In searching for an ana-

lytical expression valid for all positive values of  $\alpha_0$ , we make the substitution  $u = \omega t$  on the integral expression for the dressed potential  $\langle V \rangle$ , which leads us to

$$\langle V \rangle(z; \alpha_0) = \frac{V_0}{2\pi} \int_0^{2\pi} \Theta(|z + \alpha_0 \sin u| - \ell) du. \quad (6)$$

Now, by writing this integral as a sum of four integrals corresponding to the division of the domain into four equally spaced subintervals and then substituting  $y = \alpha_0 \sin u$  and collecting similar terms, one has

$$\langle V \rangle(z; \alpha_0) = \frac{V_0}{\pi} \int_{-z-\alpha_0}^{+z+\alpha_0} \frac{\Theta(|z+y| - \ell)}{\sqrt{\alpha_0^2 - y^2}} dy. \quad (7)$$

By making the substitution  $\tilde{z} = z + y$ , one has

$$\langle V \rangle(z; \alpha_0) = \frac{V_0}{\pi} \int_{z-\alpha_0}^{z+\alpha_0} \frac{\Theta(|\tilde{z}| - \ell)}{\sqrt{\alpha_0^2 - (\tilde{z} - z)^2}} d\tilde{z}. \quad (8)$$

Note in this integral that  $\langle V \rangle(z; \alpha_0) = V_0$  whenever  $|\tilde{z}| \geq \ell$ . This means that the original potential well is not altered at points with  $|z| \geq \ell + \alpha_0$  (i.e., far away from the QW interfaces). Let us then restrict our attention to the points with  $|z| < \ell + \alpha_0$ , where the laser-dressed potential in Eq. (8) can be written as

$$\langle V \rangle = \frac{V_0}{\pi} \left[ \Theta(\alpha_0 - z - \ell) \int_{z-\alpha_0}^{-\ell} \frac{d\tilde{z}}{\sqrt{\alpha_0^2 - (\tilde{z} - z)^2}} + \Theta(z + \alpha_0 - \ell) \int_{\ell}^{z+\alpha_0} \frac{d\tilde{z}}{\sqrt{\alpha_0^2 - (\tilde{z} - z)^2}} \right]. \quad (9)$$

Since, apart from an arbitrary constant of integration,  $\int dx / \sqrt{a^2 - x^2} = \arcsin(x/a)$ , then Eq. (9) simplifies to

$$\langle V \rangle(z; \alpha_0) = \frac{V_0}{\pi} \left\{ \Theta(\alpha_0 - z - \ell) \left[ \frac{\pi}{2} - \arcsin\left(\frac{\ell + z}{\alpha_0}\right) \right] + \Theta(\alpha_0 + z - \ell) \left[ \frac{\pi}{2} + \arcsin\left(\frac{z - \ell}{\alpha_0}\right) \right] \right\}. \quad (10)$$

Finally, by noting that  $\arcsin x + \arccos x = \pi/2$  rad for all  $x$  with  $|x| \leq 1$ , we have found that

$$\langle V \rangle(z; \alpha_0) = \frac{V_0}{\pi} \left[ \Theta(\alpha_0 - z - \ell) \arccos\left(\frac{\ell + z}{\alpha_0}\right) + \Theta(\alpha_0 + z - \ell) \arccos\left(\frac{\ell - z}{\alpha_0}\right) \right], \quad (11)$$

which is our main result.

Some important features of the dressed potential can be readily extracted from Eq. (11), e.g., its even parity with respect to  $z$ , for all  $\alpha_0$ , and its value at the center of the QW, i.e., null for  $\alpha_0 \leq \ell$  and  $2(V_0/\pi) \times \arccos(\ell/\alpha_0)$  for  $\alpha_0 > \ell$ . This positive value for  $\langle V \rangle$  at  $z=0$  suggests the formation of a symmetric double well for laser fields for which  $\alpha_0 > \ell$ .

As we already pointed out, all the analytical expressions found in literature for the laser-dressed potential are valid only for  $\alpha_0 \leq L/2$ .<sup>15–20,22</sup> In fact, in these works some simple analytical expressions are presented, some of them—namely,

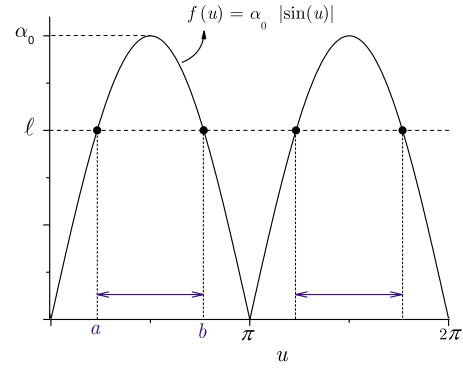


FIG. 1. (Color online) The argument of the Heaviside step function in the integrand of Eq. (6) in the case  $\alpha_0 > \ell$ . Note that the function cuts the  $\ell$ -level into two separated branches with equal lengths (horizontal arrows).

Refs. 15–17 and 20—based upon the Ehlitzky approximation, which simplifies the resolution of the integral in Eq. (6) but is unnecessary for electrons in rectangular QWs under ILFs. Let us then compare our solution to the analytical expressions presented in Refs. 18, 19, and 22. Though the expressions found in Refs. 18 and 19 involve only one  $\arccos(x)$  function and that in Ref. 22 only one  $\arcsin(x)$  function, they are essentially equivalent since they were derived for different zero-energy reference levels (in Ref. 22, the zero level is chosen at the top of the laser-free QW, whereas in Refs. 18 and 19 it is chosen at the bottom). It is then enough to analyze the expressions presented in Refs. 18 and 19, in which Niculescu and co-workers solve the definite integral in Eq. (6) analytically in terms of a single  $\arccos(x)$  function. Unfortunately, in both papers the authors have only presented the final result of the integration—see Eq. (4) in Ref. 18 and Eq. (10) in Ref. 19—without a *step-by-step solution*. It is then difficult to determine the exact point at which those authors assume the restriction  $\alpha_0 \leq L/2$  in their calculations, *but it is easy to show that they do this by comparing their solution—namely,  $(V_0/\pi) \times \arccos((\ell - |z|)/\alpha_0)$ —with the exact integral expression in Eq. (6), which can be easily solved for  $z=0$  (i.e., at the QW center). At this point, their solution yields  $(V_0/\pi) \times \arccos(\ell/\alpha_0)$  for all values of  $\alpha_0$ , instead of the correct result:*

$$\begin{aligned} \langle V \rangle(0; \alpha_0) &= \frac{V_0}{2\pi} \int_0^{2\pi} \Theta(|\alpha_0 \sin u| - \ell) du \\ &= \begin{cases} 0, & \alpha_0 \leq \ell \\ \frac{2V_0}{\pi} \times \arccos(\ell/\alpha_0), & \alpha_0 > \ell. \end{cases} \end{aligned} \quad (12)$$

In fact, when  $\alpha_0 < \ell$ , the product  $\alpha_0 \sin u$  is smaller than  $\ell$  for all values of  $u$  in the integration interval (i.e., for  $u$  from 0 to  $2\pi$ ). This nullifies the Heaviside unit step function for all values of  $u$  in this interval, and then the correct result is  $\langle V \rangle(0; \alpha_0) = 0$ . Otherwise, when  $\alpha_0 > \ell$ , one has  $|\alpha_0 \sin u| > \ell$  for all  $u$  in the subintervals  $a < u < b$  and  $\pi + a < u < \pi + b$ , where  $a = \arcsin(\ell/\alpha_0)$  and  $b = \pi - a$ . This is illustrated for  $\alpha_0 = 1.5\ell$  in Fig. 1. Therefore, the Heaviside step function evaluates to 1 in both these subintervals, remaining null out of them. Then, from Eq. (6) one has



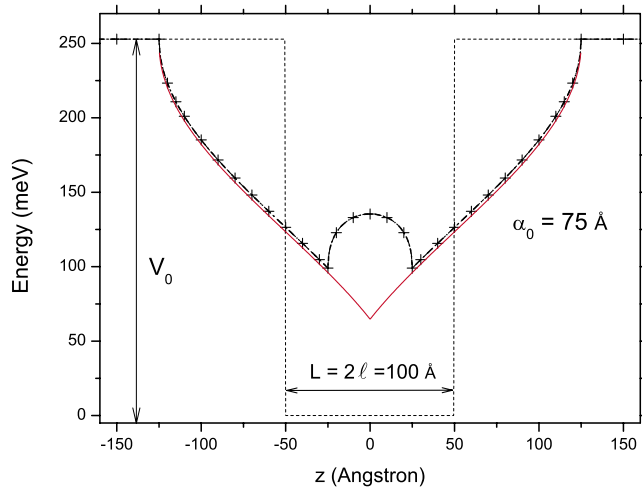


FIG. 2. (Color online) Comparison of the solutions obtained for the laser-dressed potential in the case  $\alpha_0 > \ell$ . The dashed straight lines are for the rectangular potential well in the absence of external EM fields. The points (+) are for the exact numerical integration of Eq. (6). The dash-dotted (black) line is our analytical solution, see Eq. (11). The solid (red) line is for the solution by Niculescu and co-workers (slightly shifted down for a better distinction). Here,  $\ell = 50$  Å and  $\alpha_0 = 1.5\ell$ .

$$\begin{aligned} \langle V \rangle(0; \alpha_0) &= 2 \times \frac{V_0}{2\pi} \times (b - a) = \frac{V_0}{\pi} \times (\pi - 2a) \\ &= \frac{2V_0}{\pi} \times \left( \frac{\pi}{2} - a \right) = \frac{2V_0}{\pi} \times \arccos(\ell/\alpha_0), \end{aligned}$$

in full agreement with our analytical result in Eq. (11). The fact that the “single arccos” solution by Niculescu does not work for  $\alpha_0 > L/2$  may also be confirmed graphically. In Fig. 2, it is clear that our solution agrees with the numerical integration of Eq. (6), contrarily to Niculescu’s simple expression. Note in this figure that Niculescu’s solution does not yield the “hill” on the QW center for  $\alpha_0 > L/2$ , a failure that is a consequence of the absence of one of the arccos functions that composes the correct solution, which impedes the superposition that would form the hill. We investigate the formation of the hill and its consequences in detail in the next section.

With the analytical expression for the dressed potential in Eq. (11) in hands, we find the quasistationary states by solving the following time-independent SCD equation:

$$-\frac{\hbar^2}{2m^*} \frac{d^2 \varphi(z)}{dz^2} + \langle V \rangle(z; \alpha_0) \varphi(z) = E_{KH} \varphi(z), \quad (13)$$

where  $E_{KH}$  is the energy level under ILF conditions.

### III. RESULTS AND DISCUSSION

For high-frequency, nonresonant ILFs for which  $\alpha_0 > \ell$ , our formula for the laser-dressed potential, as found in Eq. (11), suggests the formation of a symmetric double well. For investigating this possibility and its consequences on the bound states, we choose a GaAs/Al<sub>x</sub>Ga<sub>1-x</sub>As QW with  $L = 100$  Å and  $x = 0.33$  as a prototype. The conduction-band offset  $V_0$  was estimated here by taking into account Miller’s rule, i.e.,  $V_0 = 60\% \Delta E_{\text{gap}}$ , with  $\Delta E_{\text{gap}} \approx 1.155x + 0.37x^2$  (in eV).<sup>38</sup> For our QW, this yields  $V_0 = 252.87$  meV. We assume

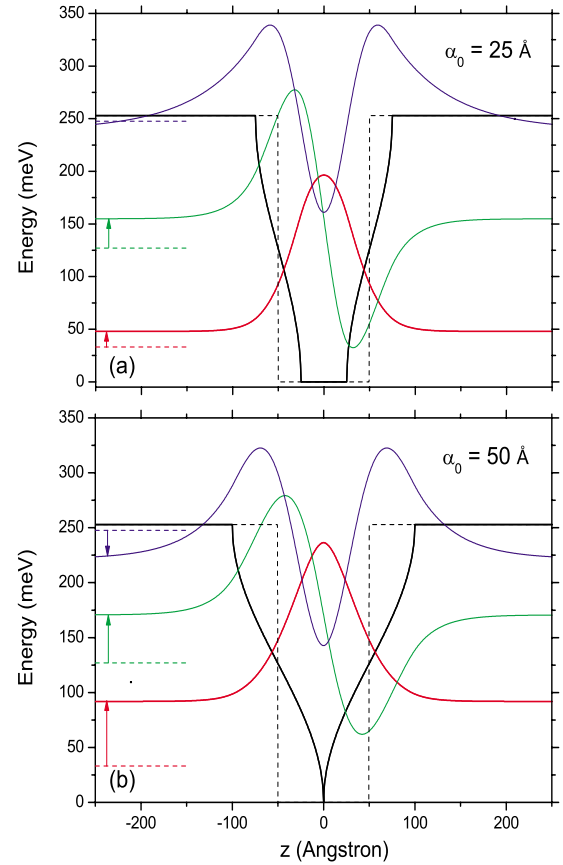


FIG. 3. (Color online) Laser-dressed potential and bound states for a GaAs/Al<sub>x</sub>Ga<sub>1-x</sub>As QW with  $x = 0.33$  and  $L = 100$  Å for (a)  $\alpha_0 = 25$  Å and (b)  $\alpha_0 = 50$  Å (for which  $\alpha_0 = L/2$ ). The dashed lines are for the laser-free QW potential. The arrows indicate the energy shifts. The wave functions are plotted upon their respective energy levels.

a uniform effective mass  $m^* = 0.067m_0$  throughout the heterostructure, where  $m_0$  is the electron rest mass. In the absence of external fields (i.e., for  $\alpha_0 = 0$ ), this QW holds three bound states with energies 33.05, 126.99, and 247.57 meV. Under ILF conditions, the potential profile is changed, and this affects each bound-state energy level distinctly, as found by solving Eq. (13) numerically. The numerical solution we employed for the resulting eigenvalue problem is based upon the finite difference method, with the accurate three-point nonuniform discretization we introduced in Ref. 39. As seen in Fig. 3, for a given  $\alpha_0$  between 0 and  $\ell$  the well width increases smoothly from  $L - 2\alpha_0$  (at the bottom) to  $L + 2\alpha_0$  (at the top). The distinct energy shifts obtained with the increase in  $\alpha_0$ , up to  $\alpha_0 = \ell$ , can be understood as follows. States with energies below  $V_0/2$  feel an effective well width smaller than  $L$ ; hence, they are blueshifted. On the other hand, states with energies above  $V_0/2$  feel an effective well width greater than  $L$ , and then they are redshifted.

The regime  $\alpha_0 > \ell$  is more complex. As it is seen in Fig. 4, the superposition of the arccos functions generates a symmetric barrier into the well layer in the form of a hill, between  $z = -\alpha_0 + \ell$  and  $z = \alpha_0 - \ell$ . Note that the width of the hill, namely,  $2\alpha_0 - L$ , increases linearly with  $\alpha_0$ . The top of the hill is always located at the center of the well (i.e., at  $z = 0$ ), where the potential evaluates to  $V_{\text{top}}(\alpha_0) = 2V_0/\pi \times \arccos(\ell/\alpha_0)$ . The bottoms are at  $z = -\alpha_0 + \ell$  and  $z = \alpha_0 - \ell$ ,

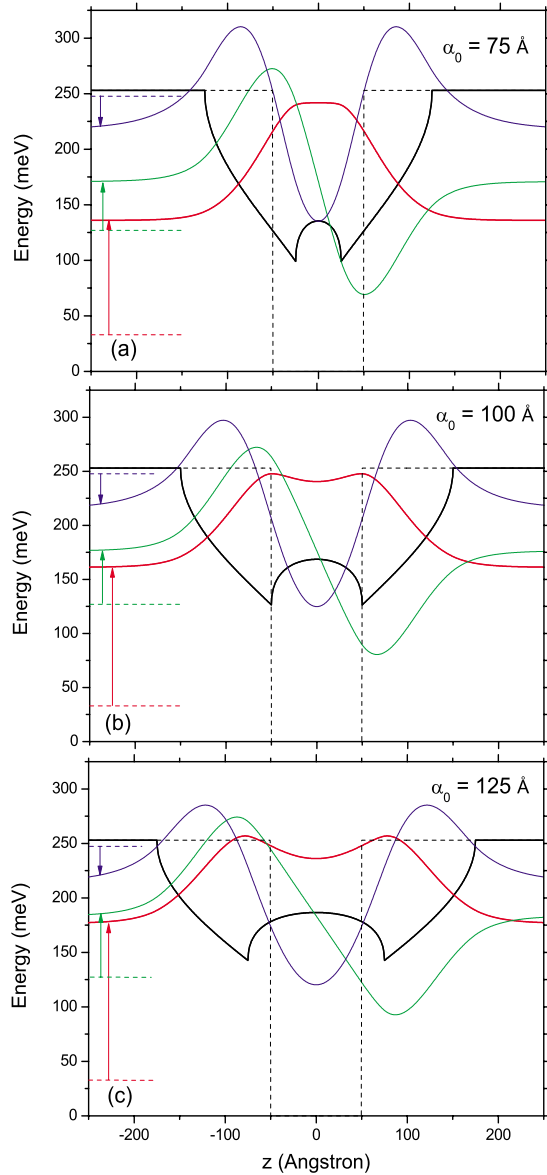


FIG. 4. (Color online) Same as in Fig. 3 for (a)  $\alpha_0=75$  Å and (b)  $\alpha_0=100$  Å (for which  $\alpha_0=L$ ) and for (c)  $\alpha_0=125$  Å (for which  $\alpha_0>L$ ). Note that the ground-state wave function gradually changes from a one- to a two-peaked function as  $E_0$  crosses down the top of the internal hill, with the increase in  $\alpha_0$ .

where the potential evaluates to  $V_0/\pi \times \arccos(2\ell/\alpha_0 - 1)$ , hence always above the bottom of the QW in the absence of external fields. It is easily seen from these expressions that both the top and the bottom tend to  $V_0$  in the large- $\alpha_0$  limit, which means that every bound-state energy level will be shifted up to  $V_0$  in this limit. Since this is also expected to take place with holes confined in the valence band,<sup>22</sup> intersubband experiments can, in principle, be developed to check if the transition energy actually tends to the  $\text{Al}_x\text{Ga}_{1-x}\text{As}$  bandgap with the increase in  $\alpha_0$ .<sup>40</sup> Also in Fig. 4, one sees that the ground-state wave function gradually changes from a one- to a two-peaked function with the increase in  $\alpha_0$ , which occurs because the rate at which  $V_{\text{top}}$  increases with  $\alpha_0$  is greater than that for  $E_0$ . With the increase in  $\alpha_0$ , the energy level  $E_0$  is surpassed by the top of the hill, and the ground-state wave function spreads in two

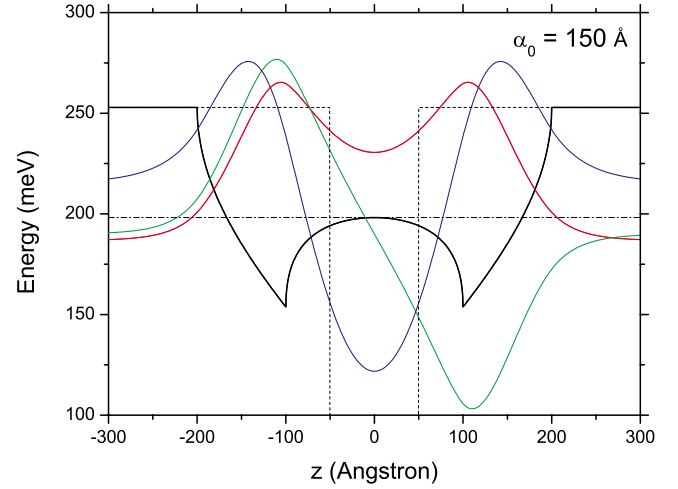


FIG. 5. (Color online) Laser-dressed potential and bound states for  $\alpha_0=150$  Å (i.e.,  $\alpha_0=3\ell$ ). The horizontal dash-dotted line marks the level of the top of the hill. Note that both  $E_0$  and  $E_1$  are below this level.

pronounced peaks. This follows directly from the structure of Eq. (13) since the second derivative of the wave functions has to be null at the points in which the dressed potential is equal to  $E_n$ . Therefore, two additional points of inflexion arise in  $\chi_n(z)$  when  $E_n$  crosses down  $V_{\text{top}}$ . This crossing also takes place for excited states, as seen in Fig. 5, in which  $\alpha_0=150$  Å (i.e.,  $\alpha_0=3\ell$ ) and the horizontal dash-dotted line marks the level of the top of the hill. We clearly see that  $V_{\text{top}}$  is above the first-excited energy level. The evolution of both the bound-state energy levels and  $V_{\text{top}}$  with the increase in  $\alpha_0$  is plotted in Fig. 6, which provides a useful guide for future experiments on intraband transitions, as well as on the transition from a single- to a double-well potential, in a semiconductor QW under ILF conditions. The lowest two energy levels ( $E_0$  and  $E_1$ ) are blueshifted with the increase in  $\alpha_0$ .

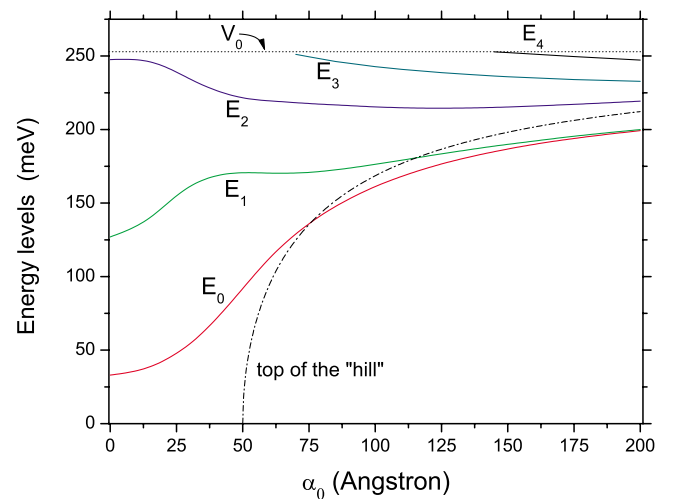


FIG. 6. (Color online) Energy levels as a function of  $\alpha_0$ . The horizontal dotted line marks the  $V_0$  level. The lowest two energy levels ( $E_0$  and  $E_1$ ) are blueshifted with the increase in  $\alpha_0$ . The third energy level ( $E_2$ ) is initially redshifted until it reaches a minimum, above which it is blueshifted. Note also the appearance of a fourth ( $E_3$ ) and a fifth ( $E_4$ ) energy level. As for  $E_2$ , they are also initially redshifted. The dash-dotted curve is for the top of the hill. Note that the curves for the energy levels  $E_0$  and  $E_1$  cross this curve with the increase in  $\alpha_0$ .

The third energy level ( $E_2$ ) is initially redshifted until it reaches a minimum for  $\alpha_0 = 125$  Å, above which it is blue-shifted. Note also the appearance of fourth ( $E_3$ ) and fifth ( $E_4$ ) energy levels for  $\alpha_0$  above 67 and 143 Å, respectively. As for  $E_2$ , they are also initially redshifted. The dash-dotted curve is for the energy of the top of the hill. Note that the energy levels  $E_0$  and  $E_1$  cross down this curve for  $\alpha_0 = 74$  Å and 112 Å, respectively. For  $\alpha_0$  above these values, two additional points of inflexion arise in the corresponding wave functions. As seen in Fig. 5, this distortion is more apparent in the ground state than in the first-excited state.

The results in Fig. 6 clearly point out to a coalescence of the bound states with the increase in  $\alpha_0$ , with the appearance of extra excited states for sufficiently large values of  $\alpha_0$ . This feature can be taken as the basis for the control of population inversion in a QW laser operating in the *optical pumping* lasing scheme, in which the proximity among the excited states is taken into account for the enhancement of the rate of population inversion.

Additionally, the emergence of a double well in the GaAs layer, for  $\alpha_0 > \ell$ , opens the possibility of creating controllable resonant states located in the well material only, distinctly from the resonance found in usual semiconductor double QWs, which is more difficult to tune since each desired resonance demands the growth of another heterostructure.<sup>41,42</sup> As in the quantum confined Stark effect, an additional weak electrostatic field can be applied along the  $z$ -axis direction in a manner that will break the symmetry and induce a small difference between the energy levels in the quantum states bounded in each side of our laser-dressed potential, thus producing an efficient tuning mechanism for this resonance process. This suggests the possibility of designing a double-well resonant tunnel diode with controllable characteristics, an interesting prediction of our theory that seems to be easily testable.<sup>42,43</sup>

## IV. CONCLUSIONS

In this work, we investigated how the potential and the corresponding bound states in a single semiconductor QW are affected by a nonresonant ILF. For sufficiently high frequencies, a closed-form expression for the dressed potential valid for all  $\alpha_0 > 0$  is derived. For laser fields for which  $\alpha_0 > L/2$ , the formation of a double-well potential in the well layer is predicted. Since the width of semiconductor QWs is typically smaller than, say, 300 Å,<sup>2,3</sup>  $\alpha_0$  values above 150 Å are required for the effects predicted here to be observable. Fortunately, the current generation of FELs can provide ILFs in the frequency range of 0.2–3226 THz, with field strengths up to  $\sim 100$  kV/cm.<sup>44,45</sup> For a terahertz laser with an intensity of  $10^4$  kW/cm<sup>2</sup>, e.g., one has  $\alpha_0 = 37a_B^*$  ( $\approx 3182$  Å),<sup>46,47</sup> which makes our results testable. As the energy shifts predicted here seem to be measurable in both intraband and interband radiative processes, experimental data for transition energies as a function of the laser intensity are awaited (see Ref. 40).

The rapid approximation of the excited levels we found for GaAs/Al<sub>x</sub>Ga<sub>1-x</sub>As QWs with the increase in  $\alpha_0$  indicates the possibility of enhancing the population inversion in the

optical pumping scheme, which is interesting for the design of powerful QW lasers. The possibility of creation of resonant states into the well layer only, with a good control of the energy differences between corresponding energy levels via a weak external bias (due to the quantum confined Stark effect), is also pointed out. Therefore, our results can be useful for the design of new optoelectronic devices.

The model presented here for electrons in a single undoped QW under nonresonant ILFs also provides a theoretical foundation for further studies of carrier states under ILF conditions in other semiconductor nanostructures, such as modulation-doped QWs, wires, and dots.

## ACKNOWLEDGMENTS

Some of the authors (A.L.A.F., E.F.S.J., and O.A.C.N.) acknowledge support from CNPq (Brazilian agency) for Doctor Research Grants. One of us (F.M.S.L.) acknowledges a postdoctoral fellowship from CNPq.

- <sup>1</sup>K. Goser, P. Glosekotter, and J. Dienststuhl, *Nanoelectronics and Nanosystems* (Springer, New York, 2004).
- <sup>2</sup>C. Weisbuch and B. Vinter, *Quantum Semiconductor Structures* (Academic, Orsay, France, 1991).
- <sup>3</sup>V. V. Mitin, V. A. Kochelap, and M. A. Strosio, *Quantum Heterostructures* (Cambridge University Press, New York, 1999).
- <sup>4</sup>S. D. Ganichev and W. Prettl, *Intense Terahertz Excitation of Semiconductors* (Oxford University Press, Oxford, 2006).
- <sup>5</sup>A. P. Jauho and K. Johnsen, *Phys. Rev. Lett.* **76**, 4576 (1996); W. Xu, *Europhys. Lett.* **40**, 411 (1997); J. Kono, M. Y. Su, T. Inoshita, T. Noda, M. S. Sherwin, S. J. Allen, Jr., and H. Sakaki, *Phys. Rev. Lett.* **79**, 1758 (1997); H. Nakano, H. Kubo, N. Mori, C. Hamaguchi, and L. Eaves, *Physica E* **7**, 555 (2000); N. Mori, T. Takahashi, T. Kambayashi, H. Kubo, C. Hamaguchi, L. Eaves, C. T. Foxon, A. Patane, and M. Henini, *Physica B* **314**, 431 (2002).
- <sup>6</sup>B. G. Enders, F. M. S. Lima, O. A. C. Nunes, A. L. A. Fonseca, D. A. Agrello, F. Qu, E. F. Da Silva, Jr., and V. N. Freire, *Phys. Rev. B* **70**, 035307 (2004).
- <sup>7</sup>F. M. S. Lima, O. A. C. Nunes, A. L. A. Fonseca, M. A. Amato, and E. F. da Silva, Jr., *Semicond. Sci. Technol.* **23**, 125038 (2008).
- <sup>8</sup>R. G. Mani, J. H. Smet, K. von Klitzing, V. Narayanamurti, W. B. Johnson, and V. Umansky, *Nature (London)* **420**, 646 (2002). For a theoretical description, see J. Inarrea and G. Platero, *Phys. Rev. Lett.* **94**, 016806 (2005).
- <sup>9</sup>L. C. M. Miranda, *Solid State Commun.* **45**, 783 (1983); Y. Mizumoto, Y. Kayanuma, A. Srivastava, J. Kono, and A. H. Chin, *Phys. Rev. B* **74**, 045216 (2006).
- <sup>10</sup>O. A. C. Nunes, *J. Appl. Phys.* **58**, 2102 (1985); K. B. Nordstrom, K. Johnsen, S. J. Allen, A. P. Jauho, B. Birnir, J. Kono, T. Noda, H. Akiyama, and H. Sakaki, *Phys. Rev. Lett.* **81**, 457 (1998); S. Hughes and D. S. Citrin, *ibid.* **84**, 4228 (2000); T. Y. Zhang and W. Zhao, *Phys. Rev. B* **73**, 245337 (2006).
- <sup>11</sup>N. G. Asmar, A. G. Markelz, E. G. Gwinn, J. Cerne, M. S. Sherwin, K. L. Chapman, P. E. Hopkins, and A. C. Gossard, *Phys. Rev. B* **51**, 18041 (1995).
- <sup>12</sup>H. Hsu and L. E. Reichl, *Phys. Rev. B* **74**, 115406 (2006).
- <sup>13</sup>E. Gerck and L. C. M. Miranda, *Appl. Phys. Lett.* **44**, 837 (1984).
- <sup>14</sup>E. C. Valadares, *Phys. Rev. B* **41**, 1282 (1990); C. Zhang, *Appl. Phys. Lett.* **78**, 4187 (2001).
- <sup>15</sup>Q. Fanyao, A. L. A. Fonseca, and O. A. C. Nunes, *Phys. Status Solidi B* **197**, 349 (1996).
- <sup>16</sup>F. Qu and P. C. de Morais, *J. Phys. Soc. Jpn.* **67**, 513 (1998).
- <sup>17</sup>Q. Fanyao, A. L. A. Fonseca, and O. A. C. Nunes, *Superlattices Microstruct.* **23**, 1005 (1998).
- <sup>18</sup>E. C. Niculescu, L. M. Burileanu, and A. Radu, *Superlattices Microstruct.* **44**, 173 (2008).
- <sup>19</sup>A. Radu, E. C. Niculescu, M. Cristea, and J. Optoelectron, Adv. Mater. (Weinheim, Ger.) **10**, 2555 (2008).
- <sup>20</sup>H. Sari, E. Kasapoglu, I. Sokmen, and N. Balkan, *Semicond. Sci. Technol.* **18**, 470 (2003).

- <sup>21</sup>H. Sari, E. Kasapoglu, I. Sokmen, and M. Gunes, *Phys. Lett. A* **319**, 211 (2003); E. Kasapoglu, H. Sari, U. Yesilgul, and I. Sokmen, *J. Phys.: Condens. Matter* **18**, 6263 (2006); N. R. Das and S. Sen, *Physica B* **403**, 3734 (2008).
- <sup>22</sup>O. O. Diniz Neto and F. Qu, *Superlattices Microstruct.* **35**, 1 (2004).
- <sup>23</sup>W. Xu, *Appl. Phys. Lett.* **89**, 171107 (2006).
- <sup>24</sup>F. Ehlotzky, *Can. J. Phys.* **63**, 907 (1985); *Phys. Lett. A* **126**, 524 (1988).
- <sup>25</sup>This is a good approximation for electrons with small wavenumbers in GaAs, in which the minimum of the conduction band (at  $\mathbf{K}=0$ ) has a  $\Gamma_6$  symmetry.
- <sup>26</sup>Newton's method works well in the search for the roots of these transcendental equations.
- <sup>27</sup>The nonresonance of the laser field with the bandgap requires that  $\nu < E_{\text{gap}}/(2\pi\hbar)$ . In GaAs, this fraction evaluates to 367 THz.
- <sup>28</sup>M. H. Mittleman, *Theory of Laser-Atom Interactions* (Plenum, New York, 1982).
- <sup>29</sup>This approximation works when  $K$  and  $z$  are such that  $\exp(\pm iKz) \approx 1$ . In our QW, this reads  $KL \ll 1$ , and since  $K = \omega\eta/c$ , where  $\eta$  is the refractive index of the hosting material, one has  $\omega \ll c/(\eta L)$ . In GaAs,  $\eta = 3.3$  and then  $\nu \ll 1447$  THz for a 100 Å wide QW.
- <sup>30</sup>H. A. Kramers, *Collected Scientific Papers* (North-Holland, Amsterdam, 1956), p. 866.
- <sup>31</sup>W. C. Henneberger, *Phys. Rev. Lett.* **21**, 838 (1968).
- <sup>32</sup>The operator  $U$  can be decomposed as  $U = U_1 U_2$ , where  $U_1 = \exp[-i/\hbar(e/m^* \int \mathbf{A} \cdot \mathbf{p} dt)]$  is a translation operator and  $U_2 = \exp[-i/\hbar(e^2/2m^* \int \mathbf{A}^2 dt)]$  produces only a gauge transformation which, in the dipole approximation, can be removed by a shift in the phase of  $\psi(z, t)$ . See details in P. W. Milonni and J. R. Ackerhalt, *Phys. Rev. A* **39**, 1139 (1989).
- <sup>33</sup>The property  $\exp(\pm i/\hbar \mathbf{a} \cdot \mathbf{p}) f(\mathbf{r}) = f(\mathbf{r} \pm \mathbf{a})$  for translation operators was taken into account here.
- <sup>34</sup>F. M. S. Lima, O. A. C. Nunes, M. A. Amato, A. L. A. Fonseca, and E. F. da Silva, Jr., *J. Appl. Phys.* **103**, 113112 (2008).
- <sup>35</sup>M. Gavrila and J. Z. Kaminski, *Phys. Rev. Lett.* **52**, 613 (1984).
- <sup>36</sup>M. Gavrila, in *Atoms in Intense Laser Fields*, edited by M. Gavrila (Academic, New York, 1992).
- <sup>37</sup>In the limit  $\alpha_0 \rightarrow 0$ , it is easy to show that  $\langle V \rangle(z; \alpha_0) \rightarrow V_b(z)$  since  $V_0/(2\pi) \times \int_0^{2\pi} \Theta(|z| - \ell) du = V_0 \Theta(|z| - \ell)$ . Therefore, in this limit our expression recovers the rectangular QW profile found in the absence of external fields.
- <sup>38</sup>F. M. S. Lima, A. L. A. Fonseca, O. A. C. Nunes, and Q. Fanyao, *J. Appl. Phys.* **92**, 5296 (2002).
- <sup>39</sup>F. M. S. Lima, B. G. Enders, A. L. A. Fonseca, O. A. C. Nunes, V. N. Freire, J. A. K. Freire, G. A. Farias, and E. F. da Silva, Jr., *Phys. Status Solidi C* **1**, S215 (2004).
- <sup>40</sup>Those interested in developing such experiments must be aware that the energy bandgap in semiconductors is itself changed by ILFs, as explained in Ref. 9. The binding energy due to the electron-hole Coulombian attraction, though small, must also be taken into account.
- <sup>41</sup>The bound states at the separated wells can be easily controlled by a weak external bias.
- <sup>42</sup>D. J. Day, Y. Chung, C. Webb, J. N. Eckstein, J. M. Xu, and M. Sweeny, *Appl. Phys. Lett.* **57**, 1260 (1990); D. J. Day, R. Q. Yang, J. Lu, and J. M. Xu, *J. Appl. Phys.* **73**, 1542 (1993).
- <sup>43</sup>We plan to develop a systematic theoretical study of the response of the confined levels to a weak bias for electrons and holes confined in a semiconductor QW under ILFs in a future work.
- <sup>44</sup>E. J. Minehara, M. Sawamura, and R. Hajima, *Free Electron Lasers 2003* (Elsevier Science, New York, 2004).
- <sup>45</sup>M. Abo-Bakr, J. Feikes, K. Holldack, P. Kuske, W. B. Peatman, U. Schade, G. Wustefeld, and H.-W. Hubers, *Phys. Rev. Lett.* **90**, 094801 (2003).
- <sup>46</sup>Here,  $a_B^* \equiv \hbar^2 \epsilon_r / (m^* k e^2)$  is the effective Bohr radius under high-frequency ac fields. In GaAs, one has  $a_B^* \approx 86$  Å when the high-frequency value  $\epsilon_r = 10.90$  is adopted.
- <sup>47</sup>For a laser source with frequency  $\nu$  (in terahertz) and output power  $I$  (in kW/cm<sup>2</sup>), one has  $F_0$  (kV/cm)  $\approx 0.868 \sqrt{I/\sqrt[4]{\epsilon_r}}$ , and  $\alpha_0$  (in  $a_B^*$ )  $\approx 7.31 \epsilon_r^{-5/4} \sqrt{I/\nu^2}$ .